THE JOURNAL OF PHYSICAL CHEMISTRY Letters

Letter

Cite This: J. Phys. Chem. Lett. 2018, 9, 6511−6516

pubs.acs.org/JPCL

Molecular Emission near Metal Interfaces: The Polaritonic Regime

Joel Yuen-Zhou,*[,†] Semion K. Saikin,[‡,§] and Vinod M. Menon[∥]

[†]Department of Chemistry and Biochemistry, University of California San Diego, La Jolla, California 92093, United States

[‡]Department of Chemistry and Chemical Biology, Harvard University, Cambridge, Massachusetts 02138, United States

[§]Institute of Physics, Kazan Federal University, Kazan 420008, Russian Federation

[∥]Department of Physics, Graduate Center and City College of New York, City University of New York, New York, New York 10016, United States

Supporting Information

ABSTRACT: The strong coupling of a dense layer of molecular excitons with surface-plasmon modes in a metal gives rise to polaritons (hybrid light−matter states) called plexcitons. Surface plasmons cannot directly emit into (or be excited by) free-space photons due to the fact that energy and momentum conservation cannot be simultaneously satisfied in photoluminescence. Most plexcitons are also formally nonemissive, even though they can radiate via molecules upon localization due to disorder and decoherence. However, a fraction of them are bright even in the presence of such deleterious processes. In this Letter, we theoretically discuss the superradiant emission properties of these bright plexcitons, which belong to the upper energy branch and reveal huge photoluminescence enhancements compared to bare excitons, due to near-divergences in the density of photonic modes available to them. Our study generalizes the well-known problem of molecular emission next to a metal interface to the polaritonic regime.

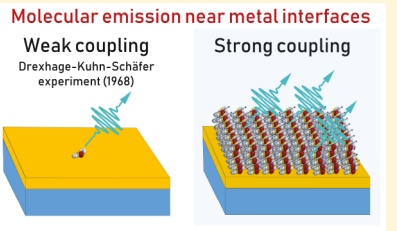

The study of molecular photoluminescence (PL) next to a metal−dielectric interface dates back to a classic experiment reported by Drexhage, Kuhn, and Schäfer (DKS) almost 50 years ago.[1,2] By controlling the distance between a molecular emitter and a metal−mirror film, the aforementioned authors showed that the observed PL rate oscillated and then monotonically increased for short distances. These oscillations were attributed to interferences between the free-space and reflected light from the mirror, and the monotonic decay was associated with irreversible energy transfer to surface plasmons (SPs) in the metal. These observations were later fully elucidated in a theory provided by Chance, Prock, and Silbey (CPS)[3,4] by adapting the results of an even older problem of antenna radiation next to the surface of the Earth, whose mathematical solution was offered by Sommerfeld as early as 1909.[5] This problem has been revisited countless times to understand molecular energy transfer processes in condensed phases.

In this Letter, we study a variation of the aforementioned problem, which offers new phenomenology that, as far as we are aware, has not been reported before. We study PL originating from (delocalized) molecular excited states (excitons) when they are strongly coupled to a SP metal film (see Figure 1). We consider a layer of $N_xN_yN_z$ molecules (of thickness W_z) placed on top of a thin dielectric spacer (of thickness z_0), which is on a thick metal film. When the molecular layer is sufficiently dense, the energy transfer between the exciton and SP modes is reversible and faster than each of the decay rates.[6,7] The resulting eigenmodes are no longer purely plasmonic or excitonic but rather polaritonic,

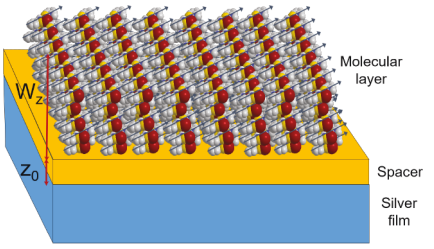

Figure 1. Plexciton setup. A molecular layer of thickness W_z sits on top of a thin dielectric spacer of thickness z_0, which in turn is placed on a metal film. Strong coupling between excitons in the molecular layer and SPs in the metal film imply that energy exchange between the excitons and SPs is much faster than their respective decay processes, giving rise to polaritonic excitations called plexcitons. Reprinted (adapted) with permission from *ACS Photonics* **2018**, *5* (1), 167−176. Copyright 2018 American Chemical Society.

being coherent superpositions of such modes. Polaritons arising from SPs and excitons are termed *plexcitons*.[8−13] As with any polaritonic system, the transmission spectrum of the plexciton system at the wavevector giving rise to resonance between the uncoupled exciton and SP bands shows a Rabi splitting (anticrossing) between two new bands,[7,8] named *upper* and *lower* plexcitons (UPs, LPs),[9,14] according to their energy ordering. Molecular polaritons have recently been the subject of intense investigation as they offer new ways for

Received: September 27, 2018
Accepted: October 29, 2018
Published: October 29, 2018

DOI: 10.1021/acs.jpclett.8b02980
J. Phys. Chem. Lett. 2018, 9, 6511−6516

coherent control of molecular processes[15] such as changes on reaction rates and thermodynamics by "imprinting" electromagnetic coherence directly onto few-[16−21] or many-molecule[22−31] ensembles (in this Letter, we will be concerned with the latter). They also provide new platforms to induce remote energy transfer[32−34] and to recreate exotic topological[12,35] and many-body phenomena at room temperature in tabletop experiments.[36−39] In this study, we highlight superradiant properties[40,41] that plexcitons exhibit that are not encountered in the weak coupling regime of a bare molecule next to a metal surface. These properties can potentially be harnessed for light harvesting and energy routing purposes in molecular materials and device applications.

We first briefly lay out a quantum-mechanical formalism to describe the plexciton system (see details in the Supporting Information, SI-I, II). Writing the Hamiltonian as $H = \sum_{\boldsymbol{k}} H_{\boldsymbol{k}}$, where the sum runs over a discrete set of in-plane (two-dimensional) exciton wavevectors $\boldsymbol{k}$, we have[6,7]

$$H_{\boldsymbol{k}} = \hbar\omega_{\boldsymbol{k}}^{\mathrm{SP}} a_{\boldsymbol{k}}^{\dagger} a_{\boldsymbol{k}} + \hbar\omega_{\mathrm{e}} \sigma_{\boldsymbol{k}}^{\dagger} \sigma_{\boldsymbol{k}} + (\mathcal{J}_{\boldsymbol{k}} \sigma_{\boldsymbol{k}}^{\dagger} a_{\boldsymbol{k}} + \mathrm{h.c.}) + H_{\mathrm{dark},\boldsymbol{k}} + H_{\mathrm{umklapp},\boldsymbol{k}} \tag{1}$$

Here, $\hbar\omega_{\boldsymbol{k}}^{\mathrm{SP}}$ and $a_{\boldsymbol{k}}^{\dagger}(a_{\boldsymbol{k}})$ [$\hbar\omega_{\mathrm{e}}$ and $\sigma_{\boldsymbol{k}}^{\dagger}(\sigma_{\boldsymbol{k}})$] are the energy and creation (annhilation) operator of a $\boldsymbol{k}$th SP [exciton]; $\mathcal{J}_{\boldsymbol{k}}$ is the collective SP−exciton coupling. $H_{\mathrm{dark},\boldsymbol{k}}$ describes dark excitons at the bare exciton energy $\hbar\omega_{\mathrm{e}}$, which do not couple directly to SPs;[27] we disregard $H_{\mathrm{umklapp},\boldsymbol{k}}$ as a negligible off-resonant contribution due to coupling with high-wavevector SP modes. Ignoring also $H_{\mathrm{dark},\boldsymbol{k}}$ for the time-being (we will discuss it at the end of the letter), $H_{\boldsymbol{k}}$ in eq 1 becomes a two-level system for every $\boldsymbol{k}$ and can be diagonalized to yield two plexciton (polariton) states of the form $|y_{\boldsymbol{k}}\rangle = [\zeta_{y_{\boldsymbol{k}}}^{(\mathrm{SP})} a_{\boldsymbol{k}}^{\dagger} + \zeta_{y_{\boldsymbol{k}}}^{(\mathrm{exc})} \sigma_{\boldsymbol{k}}^{\dagger}]|\mathrm{vac}\rangle$ with eigenenergies $\hbar\omega_{y_{\boldsymbol{k}}}$, where $y = \pm$ are labels for the UP (LP), and $|\mathrm{vac}\rangle = |\mathrm{g};0_{\mathrm{SP}};0_{\mathrm{UHP}}\rangle$ is the tensor product of the ground state for the molecular degrees of freedom ($|\mathrm{g}\rangle$), and the vacuum for the SP modes ($|0_{\mathrm{SP}}\rangle$) and the upper-half-plane (UHP) radiative modes ($|0_{\mathrm{UHP}}\rangle$); see Figure 2a.

Figure 2a shows a dispersion energy plot for the exciton, SP, and resulting plexciton bands assuming $\omega_{\mathrm{e}} = 3$ eV, $|\boldsymbol{\mu}_{eg}| = 10$ Debye, and relative permittivities $\epsilon_d = 1.3$ and $\epsilon_m(\omega) = 3.7 - \frac{(8.6\ \mathrm{eV})^2}{\omega^2}$ for the molecular (dielectric) layer and metal film, respectively. We used $\rho = 10^9$ molecules/μm^{-3}, $z_0 = 1$ nm, and $W_z = 200$ nm to account for representative parameters in the literature.[6] We took isotropic averages of $\mathcal{J}_{\boldsymbol{k}}$ to describe a molecular layer with orientational disorder.[42] Conservation of energy and in-plane momentum constrain the allowed PL processes: an excitation of frequency ω and in-plane wavevector $\boldsymbol{k}$ must output a propagating photon with the same properties. This means that for PL to occur there needs to be a real-valued k_{zd} satisfying

$$\omega = \frac{c}{\sqrt{\epsilon_d}} \sqrt{|\boldsymbol{k}|^2 + |k_{zd}|^2} \tag{2}$$

It is well-known that this is not a possibility for SP modes,[43] whose dispersion is to the right of the "light-line", $\omega_{\boldsymbol{k}}^{\mathrm{SP}} < \omega_{\boldsymbol{k}}^{\mathrm{ll}} \equiv \frac{c}{\sqrt{\epsilon_d}}|\boldsymbol{k}|$ and, thus, must be probed by coupling to gratings[44] or nanoparticles,[45] for example. The same holds formally true for LPs ($\omega_{-_{\boldsymbol{k}}} < \omega_{\boldsymbol{k}}^{\mathrm{ll}}$) and for a subset of UPs; to distinguish them from the dark exciton states (eigenstates of $H_{\mathrm{dark},\boldsymbol{k}}$), we shall call them nonemissive states. Importantly, there is another subset of UPs that are to the left of the light-line, thus being formally bright and featuring PL (see Figure 2a). We then ask, what is the rate of PL from these UPs, and how does the bright-to-nonemissive transition occur as a function of $\boldsymbol{k}$? To answer these questions, we compute the PL rate of a state $|y_{\boldsymbol{k}}\rangle$ into the free-space radiative modes of the upper-half plane (UHP) of the plexciton setup. The corresponding Wigner−Weiskopf expression (Fermi golden rule) is[46,47]

$$\gamma_{y_{\boldsymbol{k}}} = \frac{2\pi}{\hbar} \sum_{\boldsymbol{K},\chi} |\langle \mathrm{vac};\ (\boldsymbol{K},\chi)_{\mathrm{UHP}}|H_{\mathrm{int}}|y_{\boldsymbol{k}};\ 0_{\mathrm{UHP}}\rangle|^2 \times \delta(\hbar\omega_{y_{\boldsymbol{k}}} - \hbar\omega_{\boldsymbol{K}}^{\mathrm{UHP}}) \tag{3}$$

where $H_{\mathrm{int}} = -\sum_{\boldsymbol{n}\boldsymbol{s}} \hat{\boldsymbol{\mu}}_{\boldsymbol{n}\boldsymbol{s}} \cdot \hat{\mathcal{E}}_{\mathrm{UHP}}(\boldsymbol{r}_{\boldsymbol{n}\boldsymbol{s}})$ contains the interaction between each of the molecules in the slab and the electric field at the UHP. The matrix element couples an initial state with a plexciton and no UHP photons $|y_{\boldsymbol{k}};0_{\mathrm{UHP}}\rangle$ with a final state featuring no plexcitons and an UHP photon with energy $\hbar\omega_{\boldsymbol{K}}^{\mathrm{UHP}} = \frac{\hbar c|\boldsymbol{K}|}{\sqrt{\epsilon_d}}$, $|\mathrm{vac};\ (\boldsymbol{K},\chi)_{\mathrm{UHP}}\rangle = b_{\boldsymbol{K},\chi}^{\dagger}|\mathrm{vac};\ 0_{\mathrm{UHP}}\rangle$, where $b_{\boldsymbol{K}\chi}^{\dagger}$ ($b_{\boldsymbol{K}\chi}$) is the creation (annhilation) operator of photons at the UHP mode with (three-dimensional) wavevector $\boldsymbol{K} = (K_x,K_y,K_{zd})$ and polarization index χ = s,p, which satisfies the

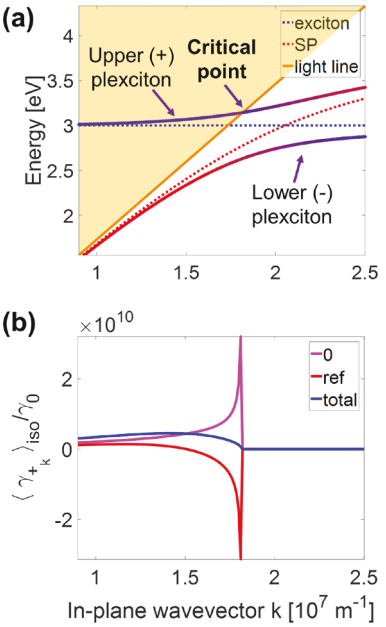

Figure 2. (a) Dispersion plot of excitations for an isotropic molecular layer. When the (flat) exciton (dashed blue) and the SP (dashed red) bands couple, they give rise to upper and lower plexcitons (UP, LP). The UP $|+_{\boldsymbol{k}}\rangle$ interpolates between the excitons and SP between $|\boldsymbol{k}| \approx 0$ and $|\boldsymbol{k}| \to \infty$; the converse is true for the LP ($|-_{\boldsymbol{k}}\rangle$). Strong hybridization occurs in the anticrossing region. The yellow shaded region contains states that emit photons, while the right region contains states that cannot due to mismatch in the energy and in-plane wavevector with respect to free-space photons. The critical point at $\boldsymbol{k} = \boldsymbol{k}^*$ separates bright and nonemissive UPs. (b) Total PL rate for the UP band $\langle\gamma_{+_{\boldsymbol{k}}}\rangle_{\mathrm{iso}} = \langle\gamma_{+_{\boldsymbol{k}},0}\rangle_{\mathrm{iso}} + \langle\gamma_{+_{\boldsymbol{k}},\mathrm{ref}}\rangle_{\mathrm{iso}}$ normalized to the single-molecule rate γ_{SM}. Contributions to $\langle\gamma_{+_{\boldsymbol{k}}}\rangle_{\mathrm{iso}}$ correspond to direct ($i = 0$) and interference terms between free-space and reflected waves (i = ref). The divergences in $\langle\gamma_{+_{\boldsymbol{k}^*},i}\rangle_{\mathrm{iso}}$ are van Hove singularities.

DOI: 10.1021/acs.jpclett.8b02980
J. Phys. Chem. Lett. 2018, 9, 6511−6516

commutation relation $[b_{\boldsymbol{K},\chi}, b^{\dagger}_{\boldsymbol{K}',\chi'}] = \delta_{\boldsymbol{K},\boldsymbol{K}'}\delta_{\chi,\chi'}$. The electric field at the UHP is given by a collection of radiative modes. Using the modal representation given by Arnoldus and George[48]

$$\hat{\mathcal{E}}_{\mathrm{UHP}}(\boldsymbol{r}) = \sum_{\boldsymbol{K},\chi} \Theta(-\boldsymbol{K}\cdot\hat{\boldsymbol{z}})\left\{\frac{(b_{\boldsymbol{K},\chi} + b_{\tilde{\boldsymbol{K}},\chi})}{\sqrt{1+|r_{\boldsymbol{K}\chi}|^2}}\sqrt{\frac{\hbar\omega_{\boldsymbol{K}}^{\mathrm{UHP}}}{2\epsilon_0\epsilon_d V}} \times[\boldsymbol{e}_{\boldsymbol{K},\chi}\mathrm{e}^{\mathrm{i}\boldsymbol{K}\cdot\boldsymbol{r}} + r_{\boldsymbol{K},\chi}\mathrm{e}^{\mathrm{i}\tilde{\boldsymbol{K}}\cdot\boldsymbol{r}}\boldsymbol{e}_{\tilde{\boldsymbol{K}},\chi}] + \mathrm{h.c.}\right\} \quad (4)$$

The radiative modes can have s or p polarization, $\boldsymbol{e}_{\boldsymbol{K},\mathrm{s}} = \frac{\boldsymbol{K}\times\hat{\boldsymbol{z}}}{|\boldsymbol{K}\times\hat{\boldsymbol{z}}|} = \frac{K_y\hat{\boldsymbol{x}} - K_x\hat{\boldsymbol{y}}}{\sqrt{K_x^2+K_y^2}}$ and $\boldsymbol{e}_{\boldsymbol{K},\mathrm{p}} = \frac{\boldsymbol{e}_{\boldsymbol{K}\mathrm{s}}\times\boldsymbol{K}}{|\boldsymbol{e}_{\boldsymbol{K}\mathrm{s}}\times\boldsymbol{K}|} = \frac{-K_{zd}(K_x\hat{\boldsymbol{x}}+K_y\hat{\boldsymbol{y}})}{|\boldsymbol{K}|\sqrt{K_x^2+K_y^2}} + \frac{\sqrt{K_x^2+K_y^2}\hat{\boldsymbol{z}}}{|\boldsymbol{K}|}$. V is the quantization volume of the UHP, Θ is the Heavyside step function, and $\tilde{\boldsymbol{K}} = \boldsymbol{K} - 2\boldsymbol{K}\cdot\hat{\boldsymbol{z}}\hat{\boldsymbol{z}}$ is the reflected wavevector for an incident wave into the metal with $K_{zd} < 0$ and Fresnel coefficients $r_{\boldsymbol{K},\mathrm{s}} = \frac{K_{zd}-K_{zm}}{K_{zd}+K_{zm}}$ and $r_{\boldsymbol{K},\mathrm{p}} = \frac{\epsilon_m K_{zd} - \epsilon_d K_{zm}}{\epsilon_m K_{zd} + \epsilon_d K_{zm}}$,[44] where $K_{zm}(\boldsymbol{K},\omega) = -\sqrt{\epsilon_m(\omega)\frac{\omega^2}{c^2} - |\boldsymbol{K}_{\perp}|^2}$. Note that although $K_{zd} \in \Re$, $K_{zm} \in \Im$ given that the UP frequency is typically below the asymptotic $k\to\infty$ SP frequency, $\omega_{\boldsymbol{K}}^{\mathrm{UHP}} < \frac{\omega_{\mathrm{p}}}{\sqrt{\epsilon_d+\epsilon_\infty}}$. This in turn yields $|r_{\boldsymbol{K}\chi}|^2=1$, i.e., lossless metals are perfectly reflective.[48]

Equation 4 implies that the rate γ_{y_k} calculated through eq 3 can be partitioned into two contributions, $\gamma_{y_k} = \gamma_{y_k,0} + \gamma_{y_k,\mathrm{ref}}$, corresponding to the direct term associated with the free-space and reflected electric fields independently and the interference term between them, as done with single-molecule calculations.[4,49,50] We present results normalized to $\gamma_{\mathrm{SM},0} = \frac{\sqrt{\epsilon_d}}{3\pi\epsilon_0\hbar}\left(\frac{\omega_{\mathrm{e}}}{c}\right)^3|\boldsymbol{\mu}_{eg}|^2$, the single-molecule PL rate in free-space, which attains a value of 0.5 ns^{-1} for the present parameters. Recall that the single-molecule PL rate scales as ω_e^3 because it can radiate across all solid angles (the number of accessible radiative modes grows as ω_e^2) and it is proportional to the intensity of the electric field ($\propto\omega_{\mathrm{e}}$).[46,47] The evaluation of eq 3 is presented in SI-III, where we also show in great detail an alternative route to obtain the same results using the dyadic Green's function formalism.[44,51,52] Here, we limit ourselves to discuss the isotropically distributed molecular layer, which already captures the essential features of the general solution; denoting isotropic averages by $\langle\cdot\rangle_{\mathrm{iso}}$, we obtain (see Figure 2b)

$$\frac{\langle\gamma_{y_{k'},i}\rangle_{\mathrm{iso}}}{\gamma_{\mathrm{SM},0}} = \left(\frac{2\pi c}{\sqrt{\epsilon_1}}\right)|\zeta_{y_k}^{(\mathrm{exc})}|^2\Theta\left(\omega_{y_k} - \frac{c}{\sqrt{\epsilon_d}}|\boldsymbol{k}|\right)\rho \times\left(\frac{\omega_{y_k}^2\frac{1}{k_{zd}}}{\omega_{\mathrm{e}}^3}\right)\frac{f_i}{\int_{z_0}^{z_{\mathrm{f}}}\mathrm{d}z\,|J_{\boldsymbol{k}}(z)|^2} \quad (5)$$

where

$$f_0 = \left|\int_{z_0}^{z_{\mathrm{f}}}\mathrm{d}z\,J_{\boldsymbol{k}}(z)\mathrm{e}^{-\mathrm{i}k_{zd}z}\right|^2 \quad (6a)$$

$$f_{\mathrm{ref}} = \frac{1}{2}\Re\left\{\left(r_{\boldsymbol{k}-k_{zd}\hat{\boldsymbol{z}},\mathrm{s}} - r_{\boldsymbol{k}-k_{zd}\hat{\boldsymbol{z}},\mathrm{p}}\frac{k_{dz}^2 - |\boldsymbol{k}|^2}{k_{dz}^2 + |\boldsymbol{k}|^2}\right) \times\left[\int_{z_0}^{z_{\mathrm{f}}}\mathrm{d}z\,J_{\boldsymbol{k}}(z)\mathrm{e}^{\mathrm{i}k_{zd}z}\right]^2\right\} \quad (6b)$$

Equations 5 and 6 are the main results of this Letter. To capture the physics behind the PL trends, we have so far considered a lossless metal. However, as we demonstrate in SI-IV, the formalism of macroscopic quantum electrodynamics (M-QED)[53−55] validates these expressions even when the metal is lossy, where $|r_{\boldsymbol{k}-k_{zd}\hat{\boldsymbol{z}},\chi}| < 1$. Let us provide a physical interpretation of these results. The PL rate for a plexciton state is proportional to its exciton population $|\zeta_{y_k}^{(\mathrm{exc})}|^2$, given that the SP population does not participate in the process. The factor of molecular density ρ signals the onset of superradiance, where the PL rate scales as the number of molecules in the coherently delocalized state, analogously to the situation in molecular aggregates.[41] Finally, the restriction given in eq 2 has two consequences in eq 5. First, Θ turns the PL off for states to the right of the light-line and, therefore, for LPs and a subset of UPs, as already discussed above. Second, for a fixed value of in-plane momentum $\boldsymbol{k}$, there are at most two possible values of out-of-plane photon wavevectors $k_{zd} = \pm\sqrt{\epsilon_d\frac{\omega_{y_k}^2}{c^2} - |\boldsymbol{k}|^2}$; therefore, the rate scales as the electric field ($\propto\omega_{y_k}$) times the density of photonic states proportional to $\left.\frac{\mathrm{d}k_{zd}}{\mathrm{d}\omega}\right|_{\omega=\omega_{y_k}} = \frac{\sqrt{|\boldsymbol{k}|^2+k_{zd}^2}}{ck_{dz}} = \frac{\omega_{y_k}}{ck_{dz}}$; this frequency scaling is drastically different from the single-molecule case, where all photon-propagation directions are available for PL. Interestingly, there is a critical in-plane wavevector $\boldsymbol{k}^* = \frac{\sqrt{\epsilon_d}\omega_{+\boldsymbol{k}^*}}{c}$ for which $k_{zd} = 0$, which coincides with the transition between bright and nonemissive UPs. This critical propagation direction is along grazing incidence, where the emitted photon travels parallel to the metal surface. At $\boldsymbol{k}^*$, $\left.\frac{\mathrm{d}k_{zd}}{\mathrm{d}\omega}\right|_{\omega=\omega_{y_{k^*}}} \to \infty$, $|\langle\gamma_{y_k,0}\rangle_{\mathrm{iso}}|, |\langle\gamma_{y_k,\mathrm{ref}}\rangle_{\mathrm{iso}}|$ diverge, yet $r_{\boldsymbol{k}^*} \to -1$ (both lossless and lossy interfaces are perfectly reflective at grazing incidence; see Figure 2). The singularities in $\langle\gamma_{y_k,i}\rangle_{\mathrm{iso}}$ are van Hove anomalies[56−59] arising from the effective one-dimensional nature of the PL process where, given a fixed in-plane momentum $\boldsymbol{k}$ dictated by the SP mode, the (one-dimensional) out-of-plane momentum k_{zd} must be chosen to conserve energy. Incidentally, as explained in ref 60, these singularities are also at the origin of the narrow resonances observed in surface lattice plasmons,[61] a phenomenon described under the umbrella of Rayleigh−Wood anomalies.[62,63] The physical origin of these collective state anomalies is thus different from single-molecule emission anomalies in quasi-one-dimensional photonic crystals,[64] but still yields substantial enhancements of PL rates ($\frac{\langle\gamma_{y_k}\rangle_{\mathrm{iso}}}{\gamma_{\mathrm{SM},0}} > 10^9$).

The strong-coupling theory above is a good description of the plexciton system when disorder Σ_{e} in the molecular excitation energies across the layer is small compared to the collective SP−exciton coupling. Quantitatively, we expect our theory to fail when $\min_y|\omega_{y_k} - \omega_{\mathrm{e}}| < \Sigma_{\mathrm{e}}$, where $\Sigma_{\mathrm{e}} \approx 10$ meV is a typical value for organic samples.[65] That is, for the

DOI: 10.1021/acs.jpclett.8b02980
J. Phys. Chem. Lett. 2018, 9, 6511−6516

phenomenology described in this Letter, SP−exciton coupling must be strong enough that the critical point (see Figure 2a) must lie above the bare exciton energy by at least Σ_e. For the parameters used in Figure 2, our theory does not hold for plexciton and dark exciton states with $|\boldsymbol{k}| < 0.9 \times 10^7\ \mathrm{m}^{-1}$, which can efficiently form superpositions of states with various $\boldsymbol{k}$ values to localize and feature $O(\gamma_{\mathrm{SM},0})$ PL rates. On the other hand, it is known that vibrational relaxation dynamics between polaritons and dark states exhibit ultrafast relaxation rates (∼50 fs).[27,66] A detailed characterization of vibrational relaxation processes in molecular polaritons is a complex task itself and beyond the scope of this work but will be irrelevant when PL rates become much faster than the latter processes, such as in our case of interest. For the time being, these estimates suffice to place constraints on the applicability of the present theory. An important observation is that, owing to vibrational relaxation, a much stronger PL is typically expected from the lower polariton branch compared to the upper one whenever the former is emissive.[67] Thus, the presently described superradiant PL afforded by UPs renders plexcitonic systems unique in terms of polariton photophysics and could be exploited to suppress photochemical pathways[68] or induce new thermodynamic equilibria.[69] From the perspective of open quantum systems, it is also interesting to inquire about the decoherence dynamics of nonstationary states of eq 1. Recent studies of the effects of incoherent light on light-harvesting systems[70,71] have concluded that the super-Ohmic character of free-space radiative modes gives rise to anomalous relaxation mechanisms (e.g., absence of pure dephasing). The formation of delocalized states via strong SP−exciton coupling should alter these mechanisms, and studying them will be the subject of future research.

Finally, we analyze other coherent effects associated with plexciton PL. Equation 6 contains finite Fourier transforms of the coupling $J_k(z)$ at the wavevector k_{zd}, which arise from interferences of emission pathways due to molecules at different heights of the layer. This implies oscillatory features of $\langle \gamma_{y_k,i} \rangle_{\mathrm{iso}}$ as a function of molecular layer thickness W_z across an $O(k_{zd}^{-1})$ range of values. As explained in the previous paragraph, our theory is valid for strong coupling and, therefore, close to the anticrossing region and the critical wavevector $\boldsymbol{k} = \boldsymbol{k}^*$; therefore, k_{dz} is typically small, and this oscillatory effect is not appreciable unless W_z is very big (>1 μm) or if ρ increases. To see this oscillatory effect, we increase the density to a maximal value of $\rho = 3.7 \times 10^{10}$ molecules/μm^3, associated with the minimum van der Waals contact distance between chromophores, and obtain Figure 3a. The inset shows results for a superradiant state $|+_{1.3\times10^7\ \mathrm{m}^{-1}}\rangle$, which exhibits PL oscillations as a function of W_z within the first 600 nm. It is also interesting to examine yet another oscillatory behavior of $\langle \gamma_{y_k,i} \rangle_{\mathrm{iso}}$ obtained by varying the spacer thickness z_0. This effect is due exclusively to interference between incident and reflected waves and, therefore, occurs when z_0 varies across photonic distances, by analogy to the aforementioned DKS[1,2] and CPS[3,4] problems. Because we want to stay in the strong-coupling regime, we keep the maximal ρ while varying z_0 up to a threshold of ∼400 nm, after which light−matter coupling becomes weak for the wavevectors of interest. Figure 3b shows the oscillatory behavior of the PL for $|+_{1.3\times10^7\ \mathrm{m}^{-1}}\rangle$ as a function of z_0.

To conclude, we have presented a comprehensive quantum formalism to study the PL properties of plexciton systems, thus

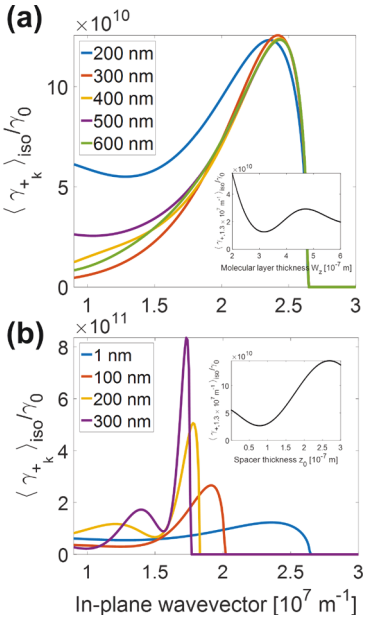

Figure 3. Normalized isotropic PL rates for the UP band $\frac{\langle \gamma_{+k} \rangle_{\mathrm{iso}}}{\gamma_{\mathrm{SM}}}$ as a function of (a) molecular layer and (b) spacer thickness, W_z and z_0, respectively. Results are presented for a maximal density of $\rho = 3.7 \times 10^{10}$ molecules/μm^3. Insets trace the PL rate for $|+_{1.3\times10^7\ \mathrm{m}^{-1}}\rangle$, which oscillates with W_z and z_0. Oscillations in (a) are due to interferences of the PL processes for molecules at different heights of the layer, while oscillations in (b) are due to reflected waves from the metal.

generalizing the paradigmatic problem of single-molecule PL next to a metal interface. We have shown that there is rich phenomenology associated with superradiance and the transition between bright and nonemissive plexciton states. Finally, we have elucidated two types of coherent effects exhibited by plexciton PL at high molecular densities. These include generalizations of the well-known PL oscillations due to reflected waves from the metal but also new coherences that arise from multiple emission pathways corresponding to different distances of the molecules from the metal layer (a result of finite thickness of the molecular layer). The described properties can be readily verified in experiments and present new control knobs to manipulate and design photophysical properties in molecular materials.

■ ASSOCIATED CONTENT

Supporting Information

The Supporting Information is available free of charge on the ACS Publications website at DOI: 10.1021/acs.jpclett.8b02980.

Surface plasmon modes: properties and quantization; derivation of the plexciton Hamiltonian eq 1; evaluation of the plexciton photoluminescence rate (Fermi golden rule and dyadic Green's function formalism); and effects of metal losses (PDF)

■ AUTHOR INFORMATION

Corresponding Author

*E-mail: joelyuen@ucsd.edu.

ORCID

Joel Yuen-Zhou: 0000-0002-8701-8793

Semion K. Saikin: 0000-0003-1924-3961

DOI: 10.1021/acs.jpclett.8b02980
J. Phys. Chem. Lett. 2018, 9, 6511−6516

Vinod M. Menon: 0000-0002-9725-6445

Notes

The authors declare no competing financial interest.

■ ACKNOWLEDGMENTS

The Abstract and TOC graphics are reprinted (adapted) with permission from *ACS Photonics* **2018**, 5 (1), 167−176. Copyright 2018 American Chemical Society. J.Y.Z. acknowledges discussions with Johannes Feist, F. J. Garcia-Vidal, Misha Fogler, Jean-Jacques Greffet, Nicholas Rivera, Matthew Du, and Raphael Ribeiro, as well as funding from NSF CAREER CHE 1654732. S.K.S. acknowledges support from the Center for Excitonics, an Energy Frontier Research Center funded by the U.S. Department of Energy under Award DE-SC0001088 and the Ministry of Education and Science of the Russian Federation for supporting the research in the framework of the state assignment, Award #3.2166.2017/4.6. V.M. acknowledges funding from the U.S. Department of Energy under Award DE-SC0017760.

■ REFERENCES

(1) Drexhage, K. H.; Kuhn, H.; Schäfer, F. P. Variation of the fluorescence decay time of a molecule in front of a mirror. *Ber. Bunsenges. Phys. Chem.* **1968**, *72*, 329−329.
(2) Drexhage, K. H. Influence of a dielectric interface on fluorescence decay time. *J. Lumin.* **1970**, *1-2*, 693−701.
(3) Chance, R. R.; Prock, A.; Silbey, R. Lifetime of an emitting molecule near a partially reflecting surface. *J. Chem. Phys.* **1974**, *60*, 2744−2748.
(4) Chance, R. R.; Prock, A.; Silbey, R. Molecular fluorescence and energy transfer near interfaces. *Adv. Chem. Phys.* **2007**, *37*, 1−65.
(5) Sommerfeld, A. Über die ausbreitung der wellen in der drahtlosen telegraphie. *Ann. Phys.* **1909**, *333*, 665−736.
(6) González-Tudela, A.; Huidobro, P. A.; Martín-Moreno, L.; Tejedor, C.; García-Vidal, F. J. Theory of strong coupling between quantum emitters and propagating surface plasmons. *Phys. Rev. Lett.* **2013**, *110*, 126801.
(7) Törmä, P.; Barnes, W. Strong coupling between surface plasmon polaritons and emitters: a review. *Rep. Prog. Phys.* **2015**, *78*, 013901.
(8) Bellessa, J.; Bonnand, C.; Plenet, J. C.; Mugnier, J. Strong coupling between surface plasmons and excitons in an organic semiconductor. *Phys. Rev. Lett.* **2004**, *93*, 036404.
(9) Fofang, N. T.; Grady, N. K.; Fan, Z.; Govorov, A. O.; Halas, N. J. Plexciton dynamics: exciton-plasmon coupling in a J-Aggregate-Au nanoshell complex provides a mechanism for nonlinearity. *Nano Lett.* **2011**, *11*, 1556−1560.
(10) Ozel, T.; Hernandez-Martinez, P. L.; Mutlugun, E.; Akin, O.; Nizamoglu, S.; Ozel, I. O.; Zhang, Q.; Xiong, Q.; Demir, H. V. Observation of selective plasmon-exciton coupling in nonradiative energy transfer: donor-selective versus acceptor-selective plexcitons. *Nano Lett.* **2013**, *13*, 3065−3072.
(11) Kochuveedu, S. T.; Kim, D. H. Surface plasmon resonance mediated photoluminescence properties of nanostructured multicomponent fluorophore systems. *Nanoscale* **2014**, *6*, 4966−4984.
(12) Yuen-Zhou, J.; Saikin, S. S.; Zhu, T.; Onbasli, M. C.; Ross, C. A.; Bulovic, V.; Baldo, M. A. Plexciton Dirac points and topological modes. *Nat. Commun.* **2016**, *7*, 11783.
(13) Bigeon, J.; Le Liepvre, S.; Vassant, S.; Belabas, N.; Bardou, N.; Minot, C.; Yacomotti, A.; Levenson, A.; Charra, F.; Barbay, S. Strong coupling between self-assembled molecules and surface plasmon polaritons. *J. Phys. Chem. Lett.* **2017**, *8*, 5626−5632.
(14) Balci, S.; Kucukoz, B.; Balci, O.; Karatay, A.; Kocabas, C.; Yaglioglu, G. Tunable plexcitonic nanoparticles: a model system for studying plasmon-exciton interaction from the weak to the ultrastrong coupling regime. *ACS Photonics* **2016**, *3*, 2010−2016.
(15) Brumer, P. W.; Shapiro, M. *Principles of the Quantum Control of Molecular Processes*; Wiley-Interscience, 2003.
(16) Galego, J.; Garcia-Vidal, F. J.; Feist, J. Cavity-induced modifications of molecular structure in the strong-coupling regime. *Phys. Rev. X* **2015**, *5*, 041022.
(17) Schmidt, M. K.; Esteban, R.; Gonzalez-Tudela, A.; Giedke, G.; Aizpurua, J. Quantum mechanical description of Raman scattering from molecules in plasmonic cavities. *ACS Nano* **2016**, *10*, 6291−6298.
(18) Chikkaraddy, R.; de Nijs, B.; Benz, F.; Barrow, S. J.; Scherman, O. A.; Rosta, E.; Demetriadou, A.; Fox, P.; Hess, O.; Baumberg, J. J. Single-molecule strong coupling at room temperature in plasmonic nanocavities. *Nature* **2016**, *535*, 127−130.
(19) Kowalewski, M.; Bennett, K.; Mukamel, S. Cavity femtochemistry: manipulating nonadiabatic dynamics at avoided crossings. *J. Phys. Chem. Lett.* **2016**, *7*, 2050−2054.
(20) Flick, J.; Ruggenthaler, M.; Appel, H.; Rubio, A. Atoms and molecules in cavities, from weak to strong coupling in quantum-electrodynamics (QED) chemistry. *Proc. Natl. Acad. Sci. U. S. A.* **2017**, *114*, 3026−3034.
(21) Szidarovszky, T.; Halasz, G. J.; Császár, A. G.; Cederbaum, L. S.; Vibók, Á. Conical intersections induced by quantum light: field-dressed spectra from the weak to the ultrastrong coupling regimes. *J. Phys. Chem. Lett.* **2018**, *0*, 6215−6223.
(22) Ebbesen, T. W. Hybrid light−matter states in a molecular and material science perspective. *Acc. Chem. Res.* **2016**, *49*, 2403−2412.
(23) Herrera, F.; Spano, F. C. Cavity-controlled chemistry in molecular ensembles. *Phys. Rev. Lett.* **2016**, *116*, 238301.
(24) Galego, J.; Garcia-Vidal, F. J.; Feist, J. Suppressing photochemical reactions with quantized light fields. *Nat. Commun.* **2016**, *7*, 13841.
(25) Baranov, D. G.; Wersall, M.; Cuadra, J.; Antosiewicz, T. J.; Shegai, T. Novel nanostructures and materials for strong light−matter interactions. *ACS Photonics* **2018**, *5*, 24−42.
(26) Sukharev, M.; Nitzan, A. Optics of exciton-plasmon nanomaterials. *J. Phys.: Condens. Matter* **2017**, *29*, 443003.
(27) Ribeiro, R. F.; Martínez-Martínez, L. A.; Du, M.; Campos-González-Angulo, J.; Yuen-Zhou, J. Polariton chemistry: controlling molecular dynamics with optical cavities. *Chem. Sci.* **2018**, *9*, 6325−6339.
(28) Flick, J.; Rivera, N.; Narang, P. Strong light-matter coupling in quantum chemistry and quantum photonics. *Nanophotonics* **2018**, *7*, 1479−1501.
(29) Groenhof, G.; Toppari, J. J. Coherent light harvesting through strong coupling to confined light. *J. Phys. Chem. Lett.* **2018**, *9*, 4848−4851.
(30) Vergauwe, R. M. A.; George, J.; Chervy, T.; Hutchison, J. A.; Shalabney, A.; Torbeev, V. Y.; Ebbesen, T. W. Quantum strong coupling with protein vibrational modes. *J. Phys. Chem. Lett.* **2016**, *7*, 4159−4164.
(31) Kolaric, B.; Maes, B.; Clays, K.; Durt, T.; Caudano, Y. Strong light−matter coupling as a new tool for molecular and material engineering: quantum approach. *Adv. Quantum Technol.* **2018**, 1800001.
(32) Zhong, X.; Chervy, T.; Zhang, L.; Thomas, A.; George, J.; Genet, C.; Hutchison, J. A.; Ebbesen, T. W. Energy transfer between spatially separated entangled molecules. *Angew. Chem., Int. Ed.* **2017**, *56*, 9034−9038.
(33) Du, M.; Martínez-Martínez, L. A.; Ribeiro, R. F.; Hu, Z.; Menon, V.; Yuen-Zhou, J. Theory for polariton-assisted remote energy transfer. *Chem. Sci.* **2018**, *9*, 6659−6669.
(34) Sáez-Blázquez, R.; Feist, J.; Fernández-Domínguez, A. I.; García-Vidal, F. J. Organic polaritons enable local vibrations to drive long-range energy transfer. *Phys. Rev. B: Condens. Matter Mater. Phys.* **2018**, *97*, 241407.
(35) Gao, W.; Li, X.; Bamba, M.; Kono, J. Continuous transition between weak and ultrastrong coupling through exceptional points in carbon nanotube microcavity exciton-polaritons. *Nat. Photonics* **2018**, *12*, 362−367.

DOI: 10.1021/acs.jpclett.8b02980
J. Phys. Chem. Lett. 2018, 9, 6511−6516

(36) Bittner, E. R.; Silva, C. Estimating the conditions for polariton condensation in organic thin-film microcavities. *J. Chem. Phys.* **2012**, *136*, 034510.
(37) Ćwik, J.; Reja, S.; Littlewood, P.; Keeling, J. Polariton condensation with saturable molecules dressed by vibrational modes. *Europhys. Lett.* **2014**, *105*, 47009.
(38) Daskalakis, K.; Maier, S.; Murray, R.; Kéna-Cohen, S. Nonlinear interactions in an organic polariton condensate. *Nat. Mater.* **2014**, *13*, 271−278.
(39) Zaster, S.; Bittner, E. R.; Piryatinski, A. Quantum symmetry breaking of exciton/polaritons in a metal-nanorod plasmonic array. *J. Phys. Chem. A* **2016**, *120*, 3109−3116.
(40) Dicke, R. H. Coherence in spontaneous radiation processes. *Phys. Rev.* **1954**, *93*, 99.
(41) Spano, F. C.; Mukamel, S. Superradiance in molecular aggregates. *J. Chem. Phys.* **1989**, *91*, 683−700.
(42) Notice that the expression for the isotropic collective coupling reported in ref 6 (two paragraphs after their equation 4) has a small error; it reads $g_{iso}^2 = \frac{2}{3}g_{\parallel}^2 + \frac{1}{3}g_{\perp}^2$, when it should read $g_{iso}^2 = \frac{1}{3}g_{\parallel}^2 + \frac{1}{3}g_{\perp}^2$. We applied this corrected formula in our calculations. See SI-II for further details.
(43) Maier, S. A. *Plasmonics: Fundamentals and Applications*; Springer, 2007.
(44) Novotny, L.; Hecht, B. *Principles of Nano-Optics*; Cambridge University Press, 2012.
(45) Aravind, P. K.; Metiu, H. Use of a perfectly conducting sphere to excite the plasmon of a flat surface. 1. Calculation of the local field with applications to surface-enhanced spectroscopy. *J. Phys. Chem.* **1982**, *86*, 5076−5084.
(46) Schatz, G. C.; Ratner, M. A. *Quantum Mechanics in Chemistry*; Dover, 2002.
(47) Scully, M. O.; Zubairy, M. S. *Quantum Optics*; Cambridge University Press, 1997.
(48) Arnoldus, H. F.; George, T. F. Spontaneous decay and atomic fluorescence near a metal surface or an absorbing dielectric. *Phys. Rev. A: At., Mol., Opt. Phys.* **1988**, *37*, 761.
(49) Ford, G. W.; Weber, W. H. Electromagnetic interactions of molecules with metal surfaces. *Phys. Rep.* **1984**, *113*, 195−287.
(50) Barnes, W. Fluorescence near interfaces: the role of photonic mode density. *J. Mod. Opt.* **1998**, *45*, 661−699.
(51) Kong, J. A. *Theory of electromagnetic waves*; Wiley-Interscience, 1975.
(52) Tai, C.-T. *Dyadic Green Functions in Electromagnetic Theory*; Institute of Electrical & Electronics Engineers (IEEE), 1994.
(53) Dung, H. T.; Knöll, L.; Welsch, D.-G. Spontaneous decay in the presence of dispersing and absorbing bodies: general theory and application to a spherical cavity. *Phys. Rev. A: At., Mol., Opt. Phys.* **2000**, *62*, 053804.
(54) Vogel, W.; Welsch, D.-G. *Quantum Optics*; John Wiley & Sons, 2006.
(55) Scheel, S.; Buhmann, S. Macroscopic quantum electrodynamics - concepts and applications. *Acta Phys. Slovaca* **2008**, *58*, 675−809.
(56) Van Hove, L. The occurrence of singularities in the elastic frequency distribution of a crystal. *Phys. Rev.* **1953**, *89*, 1189.
(57) Andreani, L. C.; Tassone, F.; Bassani, F. Radiative lifetime of free excitons in quantum wells. *Solid State Commun.* **1991**, *77*, 641−645.
(58) Cortes, C. L.; Jacob, Z. Photonic analog of a van Hove singularity in metamaterials. *Phys. Rev. B: Condens. Matter Mater. Phys.* **2013**, *88*, 045407.
(59) Remeika, M.; Leonard, J. R.; Dorow, C. J.; Fogler, M. M.; Butov, L. V.; Hanson, M.; Gossard, A. C. Measurement of exciton correlations using electrostatic lattices. *Phys. Rev. B: Condens. Matter Mater. Phys.* **2015**, *92*, 115311.
(60) García de Abajo, F. J. Colloquium: Light scattering by particle and hole arrays. *Rev. Mod. Phys.* **2007**, *79*, 1267.
(61) Zou, S.; Janel, N.; Schatz, G. C. Silver nanoparticle array structures that produce remarkably narrow plasmon lineshapes. *J. Chem. Phys.* **2004**, *120*, 10871−10875.
(62) Wood, R. W. Anomalous diffraction gratings. *Phys. Rev.* **1935**, *48*, 928.
(63) Fano, U. The theory of anomalous diffraction gratings and of quasi-stationary waves on metallic surfaces. *J. Opt. Soc. Am.* **1941**, *31*, 213−222.
(64) Viasnoff-Schwoob, E.; Weisbuch, C.; Benisty, H.; Olivier, S.; Varoutsis, S.; Robert-Philip, I.; Houdré, R.; Smith, C. J. M. Spontaneous emission enhancement of quantum dots in a photonic crystal wire. *Phys. Rev. Lett.* **2005**, *95*, 183901.
(65) Jang, S.; Dempster, S. E.; Silbey, R. J. Characterization of the static disorder in the B850 band of LH2. *J. Phys. Chem. B* **2001**, *105*, 6655−6665.
(66) Agranovich, V. M.; Litinskaia, M.; Lidzey, D. G. Cavity polaritons in microcavities containing disordered organic semiconductors. *Phys. Rev. B: Condens. Matter Mater. Phys.* **2003**, *67*, 085311.
(67) Lidzey, D. G.; Bradley, D. D. C.; Virgili, T.; Armitage, A.; Skolnick, M. S.; Walker, S. Room temperature polariton emission from strongly coupled organic semiconductor microcavities. *Phys. Rev. Lett.* **1999**, *82*, 3316−3319.
(68) Hutchison, J. A.; Schwartz, T.; Genet, C.; Devaux, E.; Ebbesen, T. W. Modifying chemical landscapes by coupling to vacuum fields. *Angew. Chem., Int. Ed.* **2012**, *51*, 1592−1596.
(69) Thomas, A.; George, J.; Shalabney, A.; Dryzhakov, M.; Varma, S. J.; Moran, J.; Chervy, T.; Zhong, X.; Devaux, E.; Genet, C.; et al. Ground-state chemical reactivity under vibrational coupling to the vacuum electromagnetic field. *Angew. Chem.* **2016**, *128*, 11634−11638.
(70) Pachón, L. A.; Botero, J. D.; Brumer, P. Open system perspective on incoherent excitation of light-harvesting systems. *J. Phys. B: At., Mol. Opt. Phys.* **2017**, *50*, 184003.
(71) Tscherbul, T. V.; Brumer, P. Long-lived quasistationary coherences in a v-type system driven by incoherent light. *Phys. Rev. Lett.* **2014**, *113*, 113601.

DOI: 10.1021/acs.jpclett.8b02980
J. Phys. Chem. Lett. 2018, 9, 6511−6516